Numerical modelling of riveted joint structures

From riveting process down to structural analysis

P.O. Bouchard[1] and P. Lasne[2]

[1]*Centre de Mise en Forme des Matériaux, Ecole des Mines de Paris, UMR 7635, BP 207, 06904 Sophia-Antipolis Cedex, France.*
URL: www-cemef.cma.fr/ e-mail: pierre-olivier.bouchard@ensmp.fr

[2]*TRANSVALOR, Parc de Haute Technologie, 694, av. du Dr. Maurice Donat, 06255 Mougins Cedex, France.*
URL: www.transvalor.com e-mail: info@transvalor.com

RÉSUMÉ. *Dans cet article, nous présentons les difficultés majeures liées à la modélisation des procédés de rivetage : contact entre corps déformables, déformations plastiques, endommagement et parfois rupture. Les logiciels éléments finis Forge2® et Forge3® permettent de modéliser des matériaux élastoplastiques ou élastoviscoplastiques en grandes déformations dans des configurations 2D et 3D. Des développements spécifiques ont été réalisés de façon à prendre en compte le contact multi-corps ainsi que pour modéliser les phases d'endommagement et de rupture. Ces développements ont été utilisés pour modéliser trois procédés de rivetage différents. Après une simulation 2D du procédé de rivetage, il est également possible d'exporter les champs mécaniques résultants sur un maillage 3D, de façon à réaliser des simlulations de tenue mécanique du point d'assemblage ainsi généré. A terme, cette technique permettra de modifier les paramètres du procédé de rivetage de façon à optimiser la résistance mécanique globale de la structur rivetée.*

ABSTRACT. *In this paper we present the main numerical difficulties to model the riveting process: contact between deformable bodies, plastic deformation, damage and sometimes fracture. Forge2® and Forge3® finite element software enable to model large deformation of elastic-plastic materials in 2D and 3D configurations. Specific developments have been performed to deal with multi-bodies contact and to model damage and fracture. They have been used to model three different riveting processes. After a 2D simulation of the riveting process, it is possible to export the mechanical fields into a 3D mesh and then to perform a 3D shearing test on the riveted structure. In the future this technique can be used to modify the riveting process parameters to optimize the structural resistance of the riveted structure.*

MOTS-CLÉS : *éléments finis, endommagement, rupture, contact multi-corps,procédé de rivetage, rivetage autopoinçonneur*

KEYWORDS: *finite element, damage, fracture, multi-bodies contatc, riveting process, self-pierce riveting*

1. Introduction

Riveted joint are widely used in the automotive or naval industry and even more in aircraft structures. Despite the importance of this joining technique, improvements of the structural behaviour of riveted joint structures are still mainly due to trial and error tests or knowledge-based procedures.

Numerical simulation can now be used to study the structural integrity of riveted joint structures. However, most of these structural analysis simulations do not take into account residual stresses, plasticity and sometimes damage due to the riveting process itself. This comes from the fact that numerical simulation of such a process is quite difficult to carry out since it involves **multimaterials contact** and **friction**. Self-pierce riveting simulation is even more difficult since the part undergoes **high plastic deformation, damage and fracture** during the process.

We propose here to study the 2D numerical modelling of **riveting** and **self-pierce riveting (SPR)**. Particular attention will be paid to the numerical modelling of damage and fracture during the self-pierce riveting process. Final results can then be exported into a 3D finite element mesh in order to study the structural resistance of the assembly in a 3D configuration.

2. Finite element software descritpion

Two finite element software, based on the same numerical technology, are used for this study. FORGE2® is used for 2D or axisymmetrical configuration, whereas FORGE3® is used for 3D simulations. Most of the time, it is possible to model the riveting process using a 2D axisymmetric simulation. Results are then exported into a 3D mesh in order to perform a 3D numerical analysis of the riveted joint.

2.1. *FORGE2® and FORGE3®*

FORGE2® and FORGE3® have been developed to model large deformation of viscoplastic, elastoplastic and elastic-viscoplastic materials. They are based on a mixed velocity-pressure formulation.

The additive decomposition of the strain rate tensor can be considered as a satisfactory approximation for usual metallic materials:

$$\dot{\varepsilon} = \dot{\varepsilon}^e + \dot{\varepsilon}^p$$

where $\dot{\varepsilon}^e$ represents the elastic part of the strain rate tensor and $\dot{\varepsilon}^p$ its plastic (or viscoplastic) part.

The elastic contribution obeys a rate form of the Hooke law:

$$\dot{\sigma} = \lambda.Trace\left(\dot{\varepsilon}^e\right)\boldsymbol{I} + 2\mu\dot{\varepsilon}^e = \boldsymbol{D^e} : \dot{\varepsilon}^e$$

where λ and μ are the usual Lamé coefficients, $\boldsymbol{I}$ is the unit (second rank) tensor and $\boldsymbol{D^e}$ is the resulting fourth rank elastic tensor.

For an elastic-plastic material, the irreversible plastic deformation is computed with the help of the von Mises plastic yield function f, defined by:

$$f(\sigma) = \frac{1}{2}\left[(\sigma_{11}-\sigma_{22})^2 + (\sigma_{22}-\sigma_{33})^2 + (\sigma_{33}-\sigma_{11})^2 + 6\sigma_{12}^2 + 6\sigma_{23}^2 + 6\sigma_{13}^2\right] - \sigma_0^2(\bar{\varepsilon})$$

Two regimes must be distinguished:

- **purely elastic deformation:**

$$\dot{\varepsilon}^p = 0 \quad if \ \ f(\sigma) < 0, \quad or \ if \ \ (f(\sigma) = 0 \ and \ \frac{\partial f}{\partial \sigma} : \dot{\sigma} < 0)$$

- **elastoplastic deformation:**

$$\dot{\varepsilon}^p = \lambda^p \frac{\partial f}{\partial \sigma} \quad if \ \ (f(\sigma) = 0 \ and \ \frac{\partial f}{\partial \sigma} : \dot{\sigma} \geq 0))$$

where the plastic multiplier λ^p is positive.

The so-called Mini-element is used in FORGE3® (Arnold *et al.*, 1984). It is based on linear isoparametric tetrahedra and a bubble function is added at element level in order to satisfy the Brezzi/Babuska condition.

The space discretization based on this element associated to the incremental formulation of the virtual work principle lead to a set of discretized non-linear equations. The well-known iterative Newton-Raphson linearization method is used. A classical one step Euler scheme is used to compute the solution at time $t+\Delta t$ when the solution at time t is known.

Besides an automatic adaptive remesher enables to deal with large deformation without losing accuracy.

2.2. *Contact treatment*

FORGE2® and FORGE3® can both handle multimaterial structures. A nodal incremental form of the penalty technique is used.

At each time step, a search of nodes that are potentially going to penetrate the opposite surface is performed. A penalty contribution, based on the penetration distance, is added to the functional for these nodes.

The contact terms arising from contact between different bodies are computed through a coupled approach based on a master-slave algorithm which deals with contact, friction and thermal conduction terms. The contact algorithm will ensure that slave nodes will not penetrate into master faces. The choice of the slave and master surfaces is based on two principal rules:

- when the mechanical behaviours of the two opposite bodies are different, the master surface is the more rigid;
- when the mechanical behaviours of the two opposite bodies are the same, it is better to have a finer mesh on the slave surface in order to minimize penetration.

The non-penetration condition will be written between a slave node and a master triangular face (introduction of fictitious element) in the current configuration. At the beginning of each time increment, a search algorithm is performed to build the node-face contact pairs which determine for all slave boundary nodes the closest master face.

More details on these techniques can be found in (Pichelin *et al.,* 2001).

2.3. *Damage model and fracture*

The use of damage mechanics is extremely important when dealing with contact joining processes based on high plastic deformation. This is particularly true for the self-pierce riveting process for which the materials undergo damage and fracture (Cf § 3.3.).

Continuum damage mechanics is a constitutive theory that describes the progressive loss of material integrity due to the propagation and coalescence of microcracks, microvoids, and similar defects. Beyond a certain value of strain, void nucleation and void growth appear in the material: this phenomenon, called damage, allows to model the ductile fracture of materials. When these voids reach a critical size, they coalesce and give raise to instabilities or cracks propagation. Damage models are generally based on the study of void growth, using different parameters such as triaxiality, maximal principal stress, plastic strain and so on.

The first models to be used were **uncoupled damage models**, which means that the damage law does not influence the mechanical properties of the material. The damage parameter is computed using an integral of a strain and stress function, and its distribution can be computed in a post-processing step. Among the numerous models, we can notice the models proposed by Cockcroft & Latham, Mc Clintock, Rice & Tracey or Oyane. See (Petrescu *et al*., 2003) for more details on these models. However, this approach can be questionable since the damage evolution does not influence the material properties.

In order to better represent the evolution of damage in materials, **coupled damage models** have been proposed. In this approach, damage and mechanical properties are directly linked and the material fracture is modeled by a progressive decrease of the global response of the structure.

Some of these models, such as the well-known Lemaitre damage model, use the notion of effective stress which represents the actual stress transmitted by the bulk material between the microdefects. A damage variable D, representing the damage level, is coupled to the mechanical behaviour of the material in order to take into account its progressive degradation.

Another frequently used approach consists in introducing a damage variable f_v

which represents the volumetric fraction of voids in the material. The parameter f_v is then used in the constitutive laws of the material and interacts with the others state variables. The damage model of Tvergaard-Needleman, based on the model introduced by Gurson belongs to these approaches (Bouchard *et al.*, 2003).

Most of these models (uncoupled and coupled) are implemented in FORGE2® and FORGE3®.

Once damage reaches a critical value, **fracture** has to be modelled. This may be accomplished using **crack propagation modeling** (Bouchard *et al.*, 2003) (Figure 1.a, b). However this fine modeling of crack propagation requires a very fine mesh at crack tips and is time consuming. It is useful when one wants to predict precisely the crack path, which is not really the case in our following simulations. An easier way to model fracture is to use the so-called **"kill-element" technique**. When the damage parameter reaches a critical value inside an element, the element mechanical contribution to the stiffness matrix is set to zero (Figure 1.c).

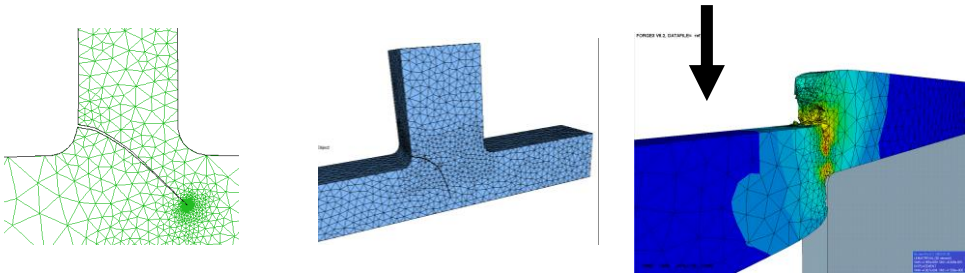

a) b) c)

Figure 1. *a) crack propagation modelling in 2D and b) in 3D configurations – c) kill-element technique during a 3D modelling of the blanking process.*

3. Applications

In the following, three different riveting processes are modelled. In the first one – hot riveting – it is interesting to notice the use of thermal dilatation to improve the structural strength of the riveted structure. In the second one – blind riveting – high plastic deformation are reached, and final results are used to study the mechanical strength of the rivet during a pull-out test. Finally, the last example deals with self-pierce riveting process. For this simulation, it is necessary to deal with damage and fracture since the rivet penetrates inti the upper sheet and then flares into the lower one. It is also shown how we can use the results of this 2D axisymmetric riveting simulation to study the strength of the riveted structure on a 3D shearing test.

3.1. *Hot riveting*

The riveting method presented here (Figure 2.) is a very old process used for naval applications. The rivets are used to seal the hull plates together. Before their positioning, rivets are heated. Then, the hammered heads of the rivets are hot deformed. The cooling induces a great clamping force between the hull plates.

To simulate this type of riveting, we consider two steps:

- the hammered head of the rivet is hot deformed after a 30 second initial cooling of a 1250°C heated part.
- a cooling stage is modelled so that the hull plates are clamped by the thermal contraction of the rivet.

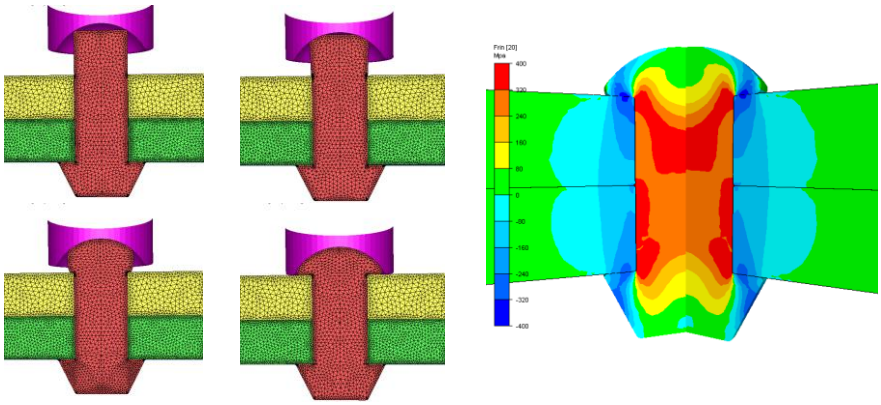

a) b)

Figure 2. *Simulation of the hot riveting process a) Forming of the hammered head of the rivet. b) Axial cramping strength after cooling of the rivet.*

The deformation of the rivets has been done considering a 2D axisymmetric assumption. The hull plates were modelled with an elastoplastic behaviour while the hot rivet had an elasto-viscoplastic behaviour. To simulate the hammer forging, an imposed velocity is given to a rigid die. A penalised contact is used to model the evolution of the contact between the hammer and the rivet including coulomb friction and thermal exchange.

The metallurgical simulation is base on a TTT diagram (Inoue *et al,* 1992; Aliaga, 2000). For the initial state, the rivet is considered as fully austenised. The incubation of ferrite, pearlite and bainite, is represented using a Scheil parameter. For the growth, a Johnson-Mehl Avrami law (Johnson *et al*, 1939) is used to compute the fraction of ferrite, pearlite or bainite transformed.

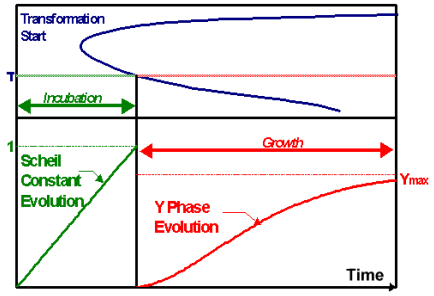

The martensitic transformation is predicted using the Koistinen Marburger law (Koistinen *et al*, 1959). The martensite volume fraction is function of the temperature when the temperature is lower than the martensite transformation temperature.

The metallurgical transformation is coupled with the thermal computation thought the transformation enthalpy of each phase.

The variation of density between the different phases induces volume changes during allotropic transformations. The transformation plasticity is also taken into account to represent the abnormal deformation created during the metallurgical transformation under stress (Gautier *et al*, 1987 ; Gautier *et al*, 1995). In this case, the decomposition of the strain rate tensor is generalize with the following equation:

$$\dot{\varepsilon} = \left[\dot{\varepsilon}^{e} + \dot{\varepsilon}^{p} + \dot{\varepsilon}^{th}\right] + \left[\dot{\varepsilon}^{tp} + \dot{\varepsilon}^{tr}\right]$$

Where

$\dot{\varepsilon}^{e}$, $\dot{\varepsilon}^{p}$, $\dot{\varepsilon}^{th}$, $\dot{\varepsilon}^{tp}$, $\dot{\varepsilon}^{tr}$ are parts of the strain rate tensor

$\dot{\varepsilon}^{e}$ for elastic deformation

$\dot{\varepsilon}^{p}$ for the deviatoric plastic (or viscoplastic) deformation

$\dot{\varepsilon}^{th}$ for the volumic thermal expansion

$\dot{\varepsilon}^{tp}$ for the deviatoric plastic transformation

$\dot{\varepsilon}^{tr}$ is the volumic transformation change

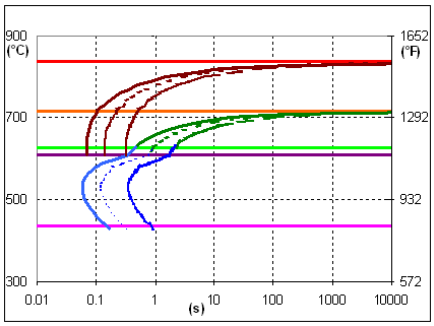

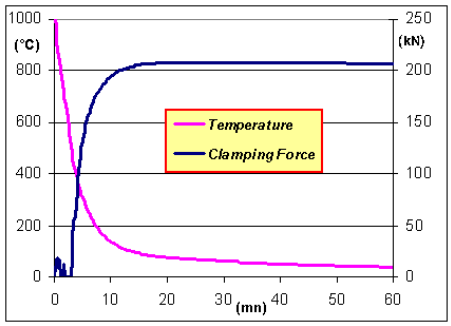

a) b)

Figure 3. a) Steel TTT diagram b)Evolution of the clamping force and the rivet temperature during cooling

3.2. *Blind riveting and pull-out test*

In this example, two sheets are riveted by bulging the collapse chamber of the rivet (See Figure 4).

Parts are already holed so that no damage and fracture model has to be used in this simulation. However a self-contact appears at the end of the process inside the collapse chamber.

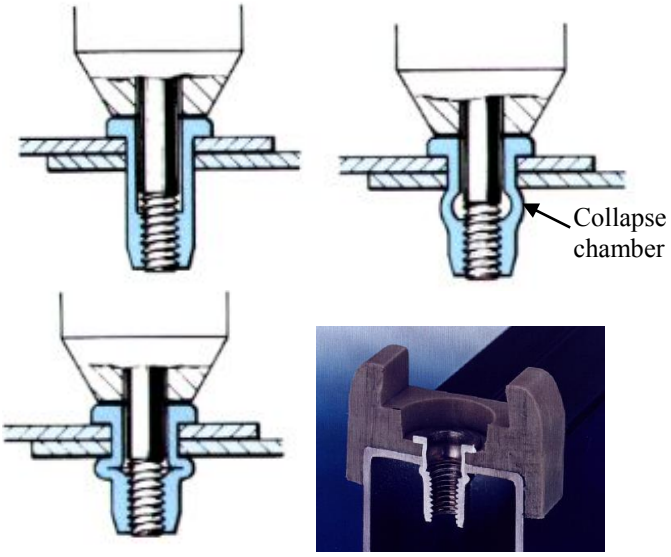

Figure 4. *Riveting process.*

The riveting process is performed in a 2D axisymmetric configuration. Materials used in this study are elastoplastic with a power hardening law and a Coulomb friction law is used at interfaces.

The numerical simulation has been performed in three steps. First the riveting process is modelled (Figure5.a). Then a stress relaxation is carried out (Figure 5.b), and finally, a pull-out test is performed in the axis of the rivet for 2D axisymmetric purposes (Figure 5.c).

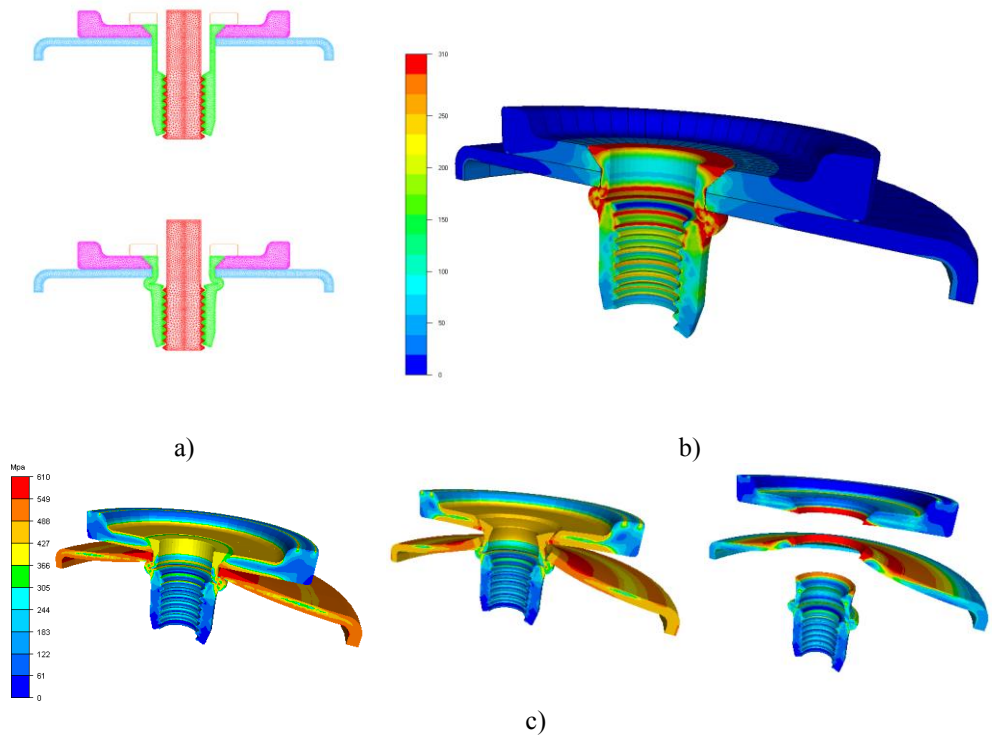

Figure 3. *a) the riveting process – b) stress relaxation – c) pull-out test.*

For the simulation of the riveting process, we consider multiple deformable bodies and the self contact in the rivet has been taken into account in order to represent the fold created during riveting

These simulation allow to obtain both the force needed for riveting and the maximum axial force possible to apply on the riveting structure.

3.3. Self-Pierce Riveting (SPR) and shearing test

3.3.1. *The SPR process*

In order to reduce the weight of vehicles structure, aluminum alloys are getting more and more used in the automotive industry. Consequently, new joining techniques, such as Self-Pierce Riveting (SPR) are used to replace Spot Welding which is not adapted to join material of different nature.

SPR technology is a relatively new fastening technique that enables to join such different metals. A punch presses a semi-tubular rivet into two (and sometimes more) sheets of metal supported by a lower die. The rivet pierces the upper sheet and penetrates into the bottom sheet which flares according to the shape of the lower die.

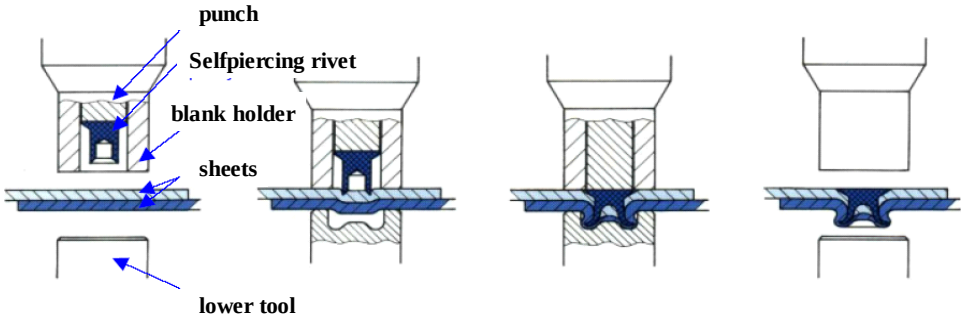

Figure 4. *Self-pierce riveting process.*

Despite the importance of this joining technique, improvements of the structural behaviour of SPR joint structures are still mainly due to trial and error tests or knowledge-based procedures. Numerical simulation can now be used to study the structural integrity of SPR joint structures. However the numerical simulation of the SPR process is particularly complex, since we have to deal with large deformation of a multimaterial structure, including damage and fracture.

3.3.2. *Numerical simulation input data*

In the following example, we show the SPR of a 1 mm upper sheet of aluminium 5754 and a 2 mm lower sheet of mild steel using a high strength steel self-pierce rivet. The three metals are considered as elastic-plastic, and we assume no strain rate and temperature dependency so that hardening is represented using a power hardening law:

$$\sigma = \sqrt{3} * \boldsymbol{K}_0 * (\varepsilon_{\boldsymbol{p}} + \varepsilon_{\boldsymbol{p}0})^{\boldsymbol{n}}$$

where σ is the equivalent stress, ε_p and ε_{p0} are respectively the plastic strain and a strain regularization term, K_0 is the consistency of the material and n is the hardening exponent.

The Lemaitre coupled damage model is used for these simulations. Materials parameters – elastic-plastic and damage – are identified by inverse analysis on a tensile test for sheets and on a compression test for the rivet.

Geometries and meshes are shown in Figure 6.a. Specific refinement boxes (Figure 6.b) are linked to the punch displacement in order to preserve a good accuracy in the pierced zone. Exact dimensions are not indicated for confidentiality purposes.

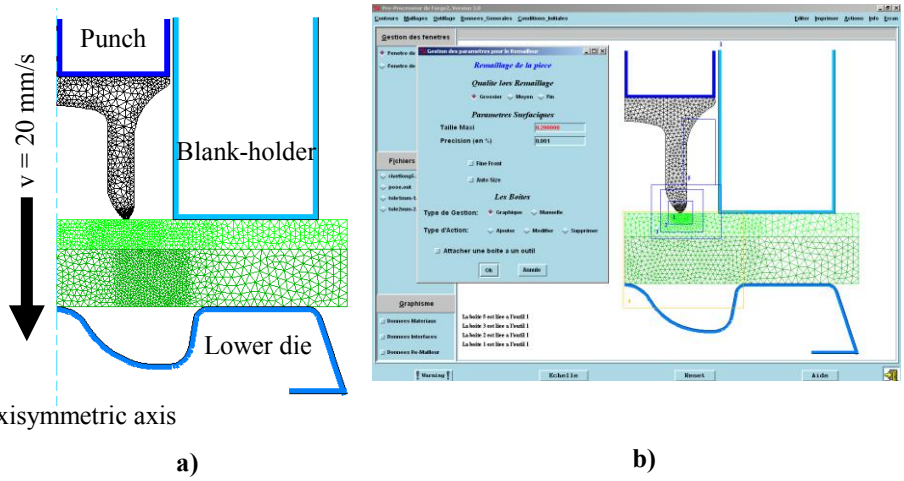

Figure 5. *a) initial mesh and geometry and b) remeshing controls.*

Friction is based on a Coulomb law limited by a Tresca coefficient.

3.3.3. *Numerical simulation results*

In figure 8, we show 4 stages of the SPR process. At first, the self-pierce rivet penetrates into the aluminium upper sheet (Figure 7.a). Then it pierces completely the aluminium sheet (Figure 7.b) and penetrates into the steel lower sheet (Figure 7.c). At this stage we can see a slight decohesion of the two sheets. Finally the rivet reaches his final position (Figure 7.d). It is interesting to see on this last stage that the lower die is not fully filled.

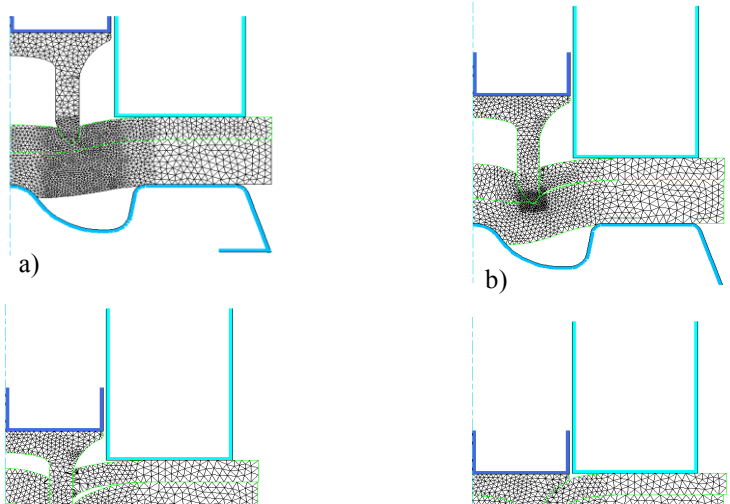

Figure 6. *Self-piercing riveting.*

It is important to highlight the fact that we can reach extremely important plastic strain during the process. However, the identification of mechanical properties on sheets have been performed using a traction test which only gives low plastic deformation. In the future, it would be better to identify the materials parameters using a piercing or a punching test.

3.3.4 Experimental validations

Validation with experiments can be performed both from a geometrical point of view and from load-displacement curves.

Figure 8.a exhibits an excellent correlation when superimposing the numerical final geometry and the experimental one. We can notice for example that the lower tool is not filled at the end of the riveting process. An optimization of the shape of this lower tool could thus reinforce the final mechanical behaviour of the rivet.

In Figure 8.b, numerical and experimental load-displacement curves are in good agreement. At the end of the process, the numerical load increase is higher than the experimental one. This comes from an overestimation of the rivet rigidity due to parameters identification on a compressive test. Consequently, the rivet does not flare enough at the end of the process. This involves an increase of the punch load due to the fact that the extremity of the rivet is very close to the lower rigid die.

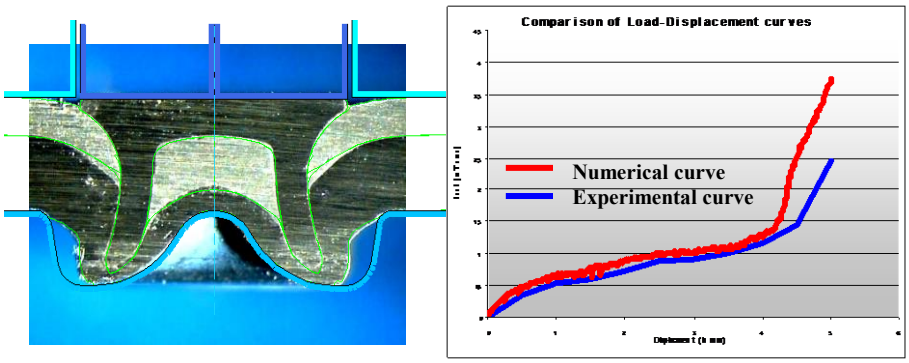

a) **b)**

Figure 7. *a) Geometrical comparison between experiment and numerical simulation – b) Comparison of numerical and experimental load-displacement curves.*

3.3.5. From the riveting process down to structural analysis

An other important issue when modelling the SPR process is to be able to study the mechanical behaviour of this joined structure.

At the end of the SPR process, it is possible to export mechanical fields (stress, strain, damage, etc…) into a 3D mesh in order to perform a 3D structural analysis. This operation is particularly complex since instead of three initial parts, we have now four different parts (the upper sheet has been split into two different parts).

This transfer is performed in three stages: first a 3D geometry is extrapolated from the 2D axisymmetric final geometrical configuration of the SPR process (Figure 9.a). Then, a new 3D mesh is generated for each part of the SPR joint (Figure 9.b). Finally, final mechanical fields (residual stresses, damage, …) of the SPR simulation are imposed as initial fields for the 3D structural analysis simulation. An interpolation technique based on proximity is used to transfer these fields from the former 2D mesh to the new 3D mesh.

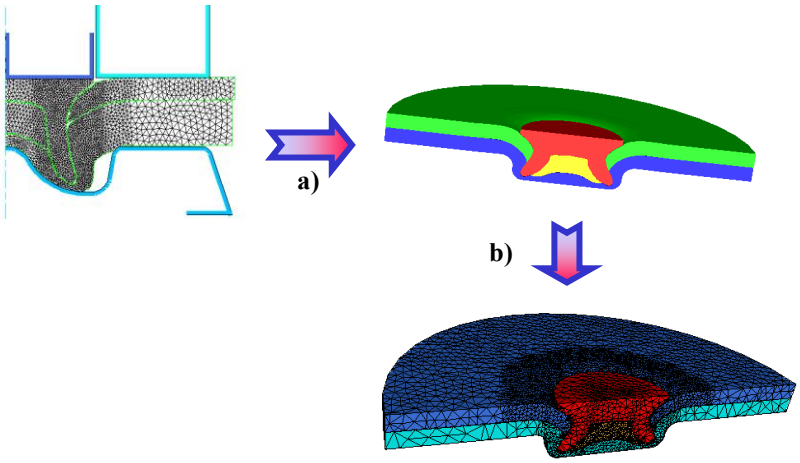

Figure 8. *Transfer from a 2D axisymmetric configuration to a 3D configuration.*

Then a 3D shearing test is performed using Forge3® as shown in figure 10.a. The numerical load-displacement curve presented in figure 11.b is in good agreement with experimental maximum loads obtained from pure traction and shear traction tests.

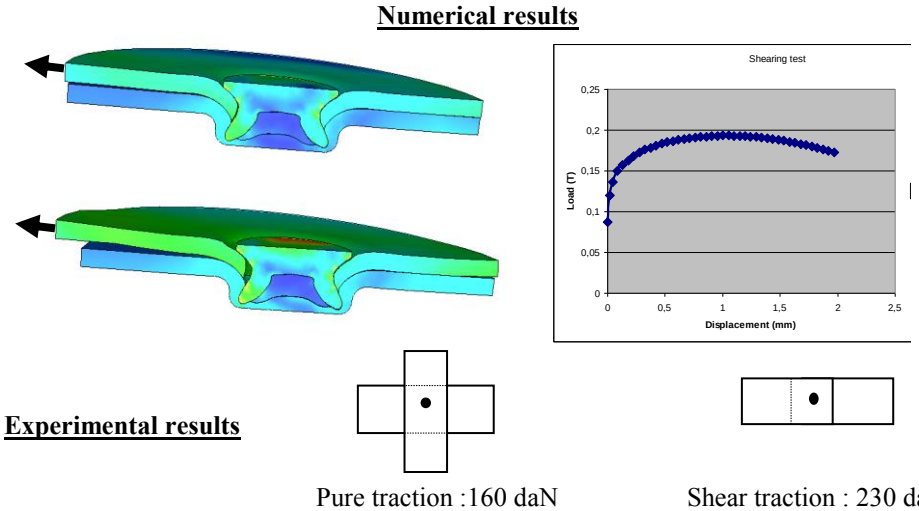

Figure 9. *Shearing test on a riveted structure.*

4. Conclusion

Numerical modelling of riveting is challenging since it involves various numerical difficulties such as damage, fracture and contact between deformable bodies. Different models have been implemented in Forge2® and Forge3® to overcome these numerical difficulties. Numerical modelling of two different riveting processes have been presented. The numerical modelling of the SPR process is the more complex one since the rivet pierces the upper sheet. A Lemaître coupled damage model and a kill-element technique have been used. Validation of the numerical simulation has been performed using geometrical comparison as well as Load-Displacement curves.

It is now possible to use the mechanical history of SPR joints in order to study their in use mechanical properties. To reach this goal, results of the 2D axisymmetric modelling of the SPR process have been exported on a 3D mesh, and a shearing mechanical test has been modelled with a good agreement with experimental results.

In the future, this methodology will enable to optimize the resistance of riveted structures since we can study the influence of riveting process parameters on its structural behaviour.

We greatly acknowledge the support of P.S.A. company for providing experimental data in support of this study.

5. Bibliographie

Aliaga C., «Simulation numérique par éléments finis de 3D du comportement thermomécanique au cours du traitement thermique d'acier : application à la trempe de pièces forgées ou coulées», *Thèse de l'Ecole Nationale Supérieure des Mines de Paris,* 28 Avril 2000.

Arnold D.N. , Brezzi F. and Fortin M., «A stable finite element for Stokes equations», Calcolo, 21, 1984, p. 337-344.

Bouchard P.O., Signorelli J., Boussetta R. and Fourment L., «Damage and Adaptive Remeshing applied to 3D modeling of blanking and Milling», *Computational Plasticity VII (COMPLAS), Barcelona*, 2003.

Bouchard P.O., Bay F. and Chastel Y., «Numerical modelling of crack propagation: automatic remeshing and comparison of different criteria», *Comput. Methods Appl. Mech. Engrg.,* 192, 2003, p. 3887-3908.

Gautier E., Simon A., Beck G.. «Plasticité de transformation durant la transformation perlitique d'un acier eutectoïde», *Acta mettalurgica, vol. 35, n°6,* 1987, p. 1367-1375.

Gautier E., Zhang J.S., Zhang X.M. «Martensitic transformation under stress in ferrous alloys. Mechanical behaviour and resulting morphologies», *Journal de physique IV*, p. 451, 1995

Inoue T., Ju D.Y. and Arimoto K. «Metallo-thermo-mechanical simulation of quenching process. Theory and computer code 'hearths'», *Proceeding of the first international conference on quenching and control of distortion, Chicago, Illinois, USA,* September 1992.

Johnson W.A. and Mehl R.F., *trans AIME, vol. 135*, 1939, p. 416

Koistinen and Marburger, «A general equation precribing exent of the austenite-martensite transformation in pure *fe – c* alloys and plain carbon steels», *Acta mettalurgica, vol 7*, 1959, p. 59-60

Petrescu D. et al., «Prediction of ductile fracture in the cold forging of steel», *ESAFORM* 2003; p. 919-922.

Pichelin E., Mocellin K., Fourment L. and Chenot J.L., «An application of a master-slave algorithm for solving 3D contact problems between deformable bodies in forming processes», *European Journal of Finite Elements*, 10, n°8, 2001, p. 857-880.